JOURNAL OF MODERN OPTICS, 1987, VOL. 34, NO. 10, 1365–1374

Rotating gratings reveal the temporal transfer function of the observing system

HELMUT GLÜNDER

Lehrstuhl für Nachrichtentechnik, Technische Universität München, Arcisstr. 21, D-8000 München 2, F. R. Germany

(*Received 16 August 1986 ; revision received*† *2 February 1987*)

Abstract. It is shown that a rotating sinusoidal grating is a useful sweep signal for the analysis of the temporal behaviour of linear imaging systems. For a suitably chosen angular velocity and spatial frequency, the spatial a.c. component of the grating appears modulated in one dimension at the output of the system. The profile of this modulation is the temporal transfer function (TTF) of the system. A quantitative analysis of this effect is presented, and results from experiments with a photographic camera are shown. It is proposed to use this method in the field of vision research since it is presently the only way to demonstrate the complex-valued TTF of the visual system for suprathreshold grating stimuli. The main consequence of the first psycho-physical investigations was the discovery of a phase reversal at the origin of the TTF of the human visual system for gratings of low spatial frequency.

1. Introduction

The rotationally symmetric, zero-order Bessel function $J_0(2\pi f_{r0} r)$, with $r = (x^2 + y^2)^{1/2}$, has an interesting Fourier transform: a δ-circle of radius f_{r0}. Thus it can be seen to be a monofrequent and isotropic function (cf. equation (A 4) in Appendix A). It is because of these properties that it is used as a stimulus pattern in vision research [1]. For this application, the Bessel pattern varies around a sufficiently high d.c. bias, thus representing a purely positive function. Such a pattern can easily be generated by incoherent optical means: a grating of sinusoidal profile (sinusoidal grating) or, more precisely, an intensity distribution of this kind, is recorded while it is rotated by multiples of 360 degrees around an axis perpendicular to the grating plane (H. Platzer, 1981, private communication). The modulation depth of the resulting pattern depends on that of the grating and on the phase shift of the grating with respect to the rotation centre (mathematical details are given in Appendix A). Of course, such a pattern can be observed directly if the angular velocity is sufficiently high that the angular motion is no longer perceived by the visual system (flicker fusion).

If a sinusoidal grating in cosine phase (figure 1) rotates by considerably less than 180 degrees around its origin in the xy-plane while it is recorded, a bar-shaped modulation is observed. It is also observable if the angular velocity is small compared

† Received in final form 25 March 1987.

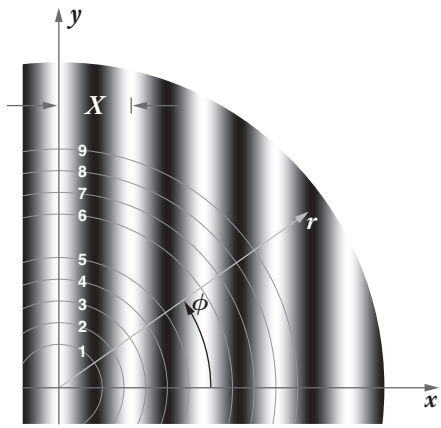

Figure 1. Scans of a cosine grating on circular paths.

with the flicker fusion frequency of the visual system. This remarkable effect, already described by Babington Smith [2] (he calls it 'band of heightened intensity'), is explained in this paper. Differing from the more phenomenological investigations of Wade [3], it is shown that the temporal transfer function (TTF) of the observing system is thereby revealed. In other words, it is demonstrated that rotating sinusoidal gratings can be used as sweep signals for the *analysis of the temporal frequency response* of imaging systems: depending on the grating frequency, sections through the (three-dimensional) spatio-temporal transfer function of a system can be produced. Practical time-dependent imaging systems show a lowpass or bandpass behaviour, i.e. they have an overall integrating characteristic. Two types of such systems must be distinguished: those for which the integration time is equal to the observation time, and those whose integration time is in general less than the observation time. The photographic camera (inter-lens shutter), as an example of the first kind, and the human visual system, as one of the second type, were analysed using this temporal sweep technique. The application of this method to the human visual system is of particular interest since, until now, its temporal behaviour could only be determined via *pointwise modulation threshold measurements* (stimuli: flickered or linearly moving gratings) which result in a *positive-valued temporal contrast sensitivity function* (CSF). The proposed sweep technique, however, allows the observation of the *entire complex-valued* TTF for an arbitrary *suprathreshold sinusoidal grating* [4].

2. Rotating gratings

A mathematical analysis is given of spatio-temporal effects associated with the observation of rotating sinusoidal gratings by temporally integrating systems. Differing from an earlier approach [5], the following treatment is based entirely on signal descriptions in the space-time domain. A vertically oriented grating in cosine phase of a spatial frequency $f = 1/X$, a mean intensity I_0, and a contrast or spatial modulation m is considered (see figure 1):

$$g(x, y) = I_0\left[1 + m\cos(2\pi x/X)\right]. \tag{1}$$

For the following mathematical derivations the grating is assumed fixed and the observing system rotates around its optical axis. The temporal signal 'seen' by a point with polar coordinates r and $\phi(t=0)=0$ in the output plane of an ideally transmitting system (TTF = const.) is

$$e(r,\phi(t)) = I_0\left[1+m\cos\psi(t)\right] \quad \text{with} \quad \psi(t) = 2\pi(r/X)\cos\phi(t). \tag{2}$$

For a constant angular velocity ω the rotation angle $\phi(t)$ is

$$\phi(t) = \omega t = 2\pi n t, \tag{3}$$

where n denotes revolutions per time unit. For $r = \text{const.}$, the output signal $e(t)$ is easily identified as a cosinusoidally phase-modulated cosine function of modulation index $2\pi r/X$. Figure 2 shows such functions for the nine radii indicated in figure 1. These plots are actual analogue recordings of the photocurrent of a small detector situated in a plane onto which a rotating grating was projected.

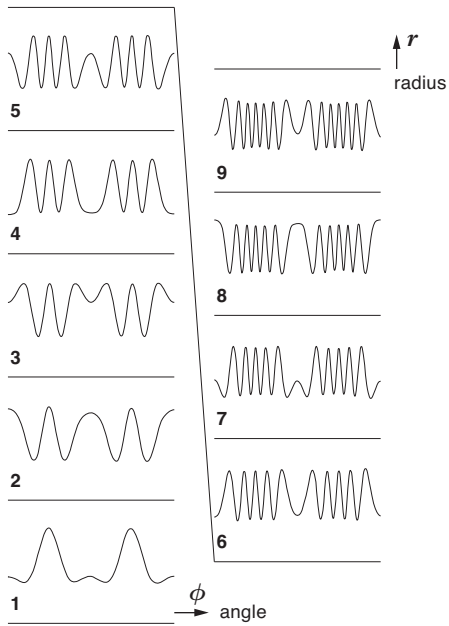

Figure 2. Phase-modulated signals from actual circular scans of a cosine grating of contrast $m \approx 0{\cdot}4$. The numbers refer to the radii indicated in figure 1 ($\Delta r = 0{\cdot}3X$). The angle ϕ runs from zero to 360 degrees.

The instantaneous angular frequency ω_{inst} of the phase-modulated signal of equation (2) is defined by

$$\omega_{\text{inst}}(r,\phi) = \mathrm{d}\psi/\mathrm{d}t = -2\pi(r/X)\omega\sin\phi, \tag{4}$$

and the instantaneous frequency in Cartesian coordinates is

$$\left|\nu_{\text{inst}}\right| = \omega y/X \quad \text{with} \quad y = r\sin\phi. \tag{5}$$

This relation between $\left|\nu_{\text{inst}}\right|$ and the coordinate y is the reason why a rotating grating is a suitable temporal sweep signal: the loci of constant instantaneous temporal frequency are parallels to the x-coordinate (see figure 1), i.e. straight lines orthogonal

to the grating lines. Thus, different temporal frequencies appear at different line-like locations.

3. Representation of temporal transfer functions

Again, the output signal at a certain point in the sensory plane of an imaging system is considered. This time, however, the system is assumed to have a TTF that is other than constant, which means that $e(t)$ is filtered, resulting in an amplitude-modulated signal. This amplitude modulation is approximately described by a signal attenuation according to the TTF at the corresponding instantaneous frequencies. According to equation (5) they appear at different parallel lines ($y = \text{const.}$), and thus the TTF of a linear space-invariant system is given by the modulation profile along the grating lines.

As with all investigations of frequency responses based on sweep techniques, the accuracy of the results increases with a decrease in the sweeping speed. This is due to the fact that the system is not tested with stationary harmonic functions but with a sweep signal approximating a temporal sequence of such functions. The quality of this approximation depends on the difference between the frequency of a stationary harmonic oscillation and the corresponding instantaneous frequency of a sweep signal (cf. Appendix B, equations (B 1)–(B 3)), i.e. on the rate of change of the instantaneous frequency:

$$\dot{\omega}_{\text{inst}} = \mathrm{d}\omega_{\text{inst}}/\mathrm{d}t = -2\pi(r/X)\omega^2\cos\phi, \tag{6}$$

or in Cartesian coordinates:

$$\dot{\omega}_{\text{inst}} = -2\pi\omega^2 x/X \quad \text{with} \quad x = r\cos\phi. \tag{7}$$

Therefore, the loci of constant error ($\dot{\omega}_{\text{inst}} = \text{const.}$) are parallels to the y-axis. The number of grating cycles $k = x/X$ within which the error is less than a certain value decreases according to the square of the inverse angular velocity. A thorough analysis, considering common lowpass systems, shows that the error is in the order of a few per cent for $k < 5$, if $\nu_0 > 30n$; where ν_0 is the temporal cut-off frequency of the lowpass and n is the frequency of rotation (see Appendix B).

4. Photographic camera

A processor for the generation of precise, sinusoidally varying gratings is sketched in figure 3 (*a*). A binary cosine-shaped template T (figure 3 (*b*)), illuminated through a ground-glass diffusor G, is 'smeared' orthogonal to its ordinate by means of a cylindrical lens system A. The resulting light distribution can be rotated by a stepper-motor-driven Dove prism DP. The grating is projected onto the screen S by the lens O. This method allows the production of high-contrast sinusoidal gratings with low total harmonic distortions ($\text{THD}_{\text{typ}} < 5$ per cent).

Figure 4 (*a*) shows a photographic recording of the light intensity in the plane of the screen for the following system parameter: $1/(2\tau n) = \nu_0/n = 16$, where τ is the exposure time (integration time). In figure 4 (*b*), the modulation profile for an ideally rectangular exposure function (figure 4 (*c*)) of an inter-lens shutter (CS in figure 3 (*a*)) is sketched. The phase shifts of 180 degrees (changes of sign) are clearly seen from figure 4 (*a*) and thus experimental evidence is given for the capability of this method to display complex TTFs.

The effect of parameter changes on the recorded pattern can be studied from the results shown in figure 5. In these experiments, τ was held constant in order to obtain

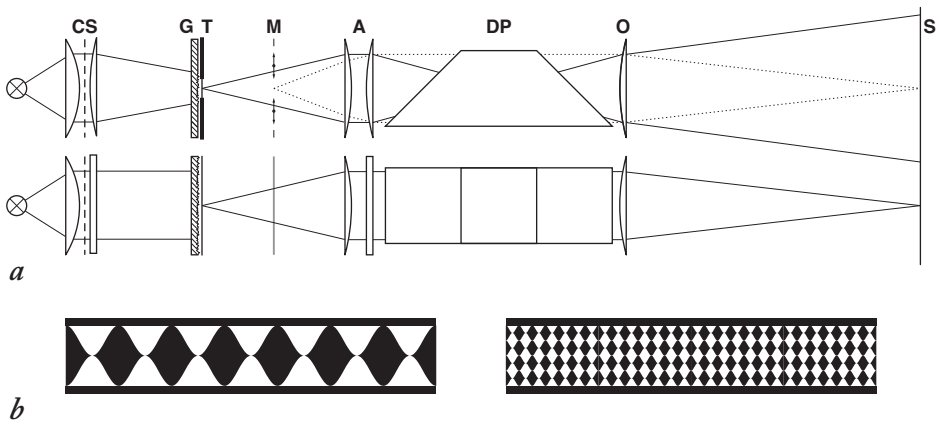

Figure 3. (*a*) Optical processor for the generation of rotating gratings and (*b*) examples of templates T that are used for the production of sinusoidal gratings.

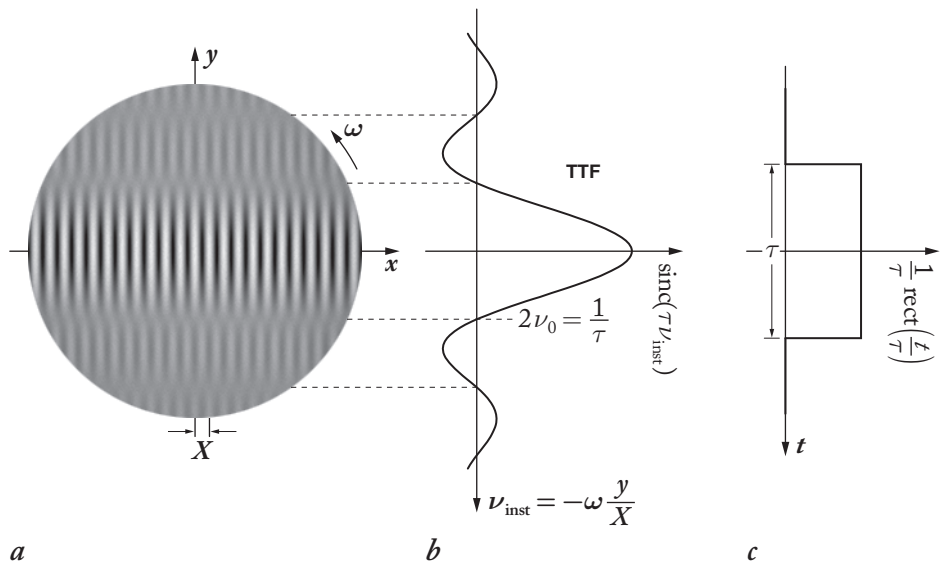

Figure 4. (*a*) Modulation exhibited by the inter-lens shutter system. (*b*) Modulation profile for (*c*) an ideally rectangular exposure function.

equal exposure conditions, while the normalized speeds of rotation $\tilde{n}$ and spatial frequencies $\tilde{f}$ of the grating were chosen as indicated. For each photograph the corresponding normalized scale factor $\tilde{y} = 1/(4\tilde{n}\tilde{f})$ is given. The loss of accuracy with increasing angular velocity and spatial frequency according to equation (7) is clear.

5. Visual system

Since we generally look at a pattern significantly longer than the integration time of our visual system, the bar-shaped modulation exhibited by a rotating grating is

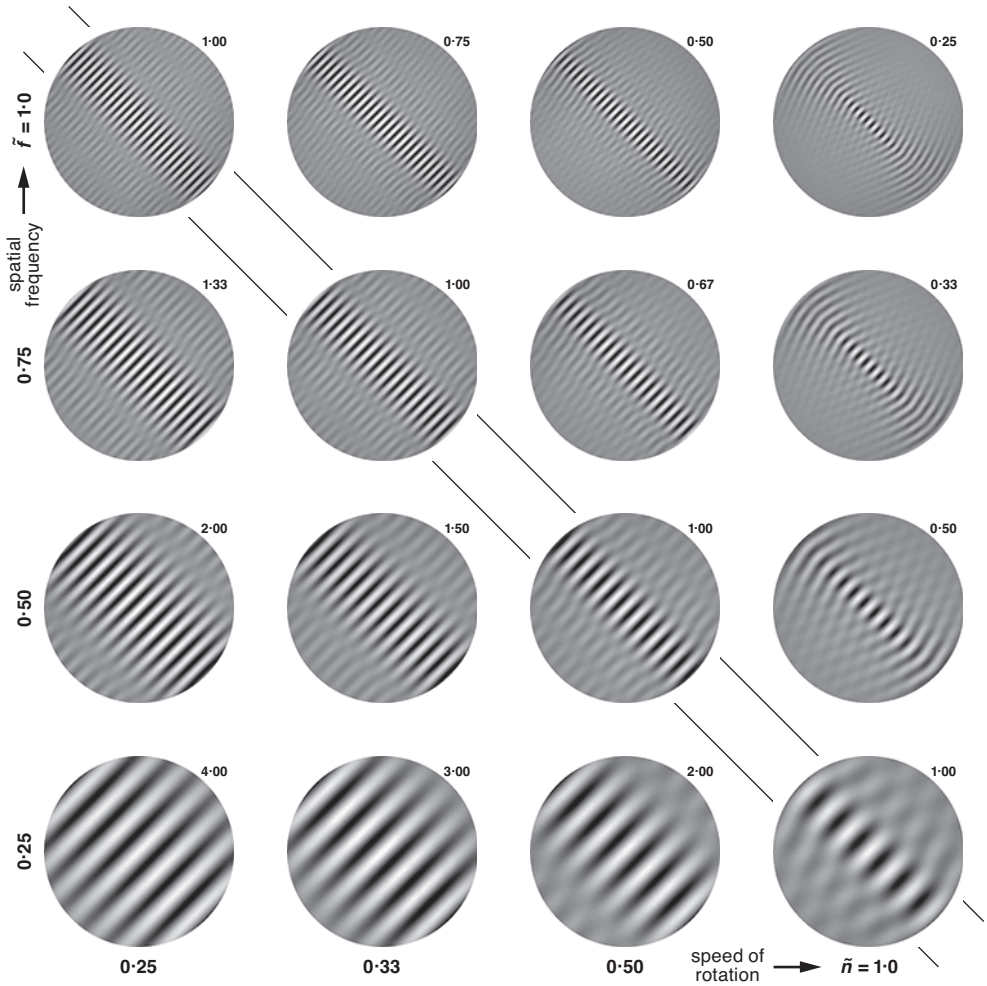

Figure 5. Effect of the parameters speed of rotation and spatial frequency on the modulation (inter-lens shutter with constant exposure time).

observed as turning at the same angular velocity as the grating itself. This makes it inconvenient to work at high frequencies of rotation. On the other hand, it is necessary to increase the frequency of rotation if the spatial frequency is decreased in order to display the entire TTF on a screen of fixed diameter or viewing angle. The latter, however, should not be too large in order to guarantee a sufficient space-invariant processing (in a global sense) [6–8].

The following rather qualitative results will, it is hoped, stimulate more extensive experiments to be performed by researchers in the field of psychophysics. In preliminary experiments the well known dependence of the flicker fusion frequency on the mean intensity [9, 10] could qualitatively be confirmed. For these investigations the experimental set-up of figure 3 (*a*) was used. A pair of line-like markers M,

oriented parallel to the template T and symmetrical to the optical axis, was introduced in the object plane of the imaging system A-O. Therefore, the markers rotated together with the grating. Subjects were able to alter the distance of the markers. For the measurements the subjects were asked to adjust the width so that the modulated area was just contained between the lines. (Another method for the measurement of the bar width is based on a masking effect described by Wade and Sanford [11, 3].) The display diameter was 3·5 degrees in a dark surround, the modulation contrast was 55 per cent, the viewing condition was binocular with natural pupil, and the subjects were asked to fixate on the centre of rotation. The mean intensity was varied between 0·1 and 10 cd m^{-2}. The change from temporal lowpass to bandpass behaviour with increasing spatial frequency and/or mean intensity (see the reviews [7, 12], and [10]) was also clearly observed. The most important result, however, was a phase shift of 180 degrees that was observed for spatial frequencies typically lower than one cycle per degree and temporal frequencies near zero (also denoted as 'shimmering effect' [3]); which confirms a recently formulated concept [13]. The effect is best observed with high intensities ($I_0 > 1$ cd m^{-2}) and very low rotational frequencies ($n < 0{\cdot}5$ s^{-1}). As soon as the grating starts revolving, the grating lines begin to shear along a line that is oriented orthogonal to the grating and passes through the centre of rotation.

In short, the unique features of this stimulus configuration and measurement technique are the feasibility to observe directly

(1) the entire TTF,
(2) magnitude and phase of the TTF,
(3) the TTF for supra-threshold modulations, and
(4) the dependence of the TTF on the grating orientation.

Furthermore, the method is based on a moving, not flickering grating, i.e. on the more natural stimulus [7].

6. Concluding remarks

While working with rotating gratings, two further useful applications were found. Even-order harmonics of gratings are easily detected if they are rotated at high angular velocities in sine phase. If a grating contains no even-order harmonics, a temporally integrating system 'sees' a constant intensity, i.e. no spatial modulation. Otherwise, radial modulations occur (for details see Appendix A). Thus, this method permits, for instance, the testing of sinusoidal gratings for their spectral purity (at least concerning even-order harmonics) and of square-wave gratings for their exact duty cycle of 1:1.

The second application is again in the field of psychophysics. Thus far, there is no consensus regarding the mechanisms that are responsible for the visibility, during or after saccadic eye movements, of structures that actually move or flicker faster than the temporal resolution of the visual system [14, 15]. The question is whether it is a tracking effect (tailing) or whether spectral components are mixed into the passband of the visual system by the high velocity of saccades (switching effect). Gratings, free from even harmonics, which rotate fast enough in sine phase so that no flicker effect and spatial modulation are observable, suddenly become visible over the *entire* display area during voluntary eye movements. This phenomenon must be due to the switching effect since rotational saccades are not known to exist.

In this paper it was demonstrated that rotating gratings are useful test patterns in

the field of optics, electro-optics and vision research. They permit a pictorial representation of the temporal transfer functions of imaging systems.

Acknowledgements

I thank H. Platzer for the initial idea and his unfailing interest in the investigations, T. Kramer for his help with the dynamic transfer functions (Appendix B), Dr R. Bamler for the highly mathematical discussions during the preparation of this paper, Professor G. Hauske and Dr T. Elsner for their advice concerning the field of psychophysics, and Dr N. J. Wade for essential hints.

Appendix A

A vertically oriented grating-like intensity distribution of the spatial frequency f_{x0}, with a phase shift $\psi_0 = 2\pi f_{x0} x_0$, a mean intensity I_0, and a contrast $0 < m \leq 1$ is given by

$$\tilde{g}(x, y) = I_0 \left\{1 + m \cos\left[2\pi f_{x0}(x - x_0)\right]\right\}, \tag{A 1}$$

and its Fourier-spectrum is

$$\begin{aligned}\tilde{G}(f_x, f_y) = I_0 \Big\{ \delta(f_x, f_y) + \tfrac{m}{2}\big[&\exp(-\mathrm{i}\psi_0)\, \delta(f_x - f_{x0}, f_y) \\ &+ \exp(+\mathrm{i}\psi_0)\, \delta(f_x + f_{x0}, f_y)\big]\Big\}.\end{aligned} \tag{A 2}$$

The phase terms in equation (A 2) are due to the phase shift ψ_0 of the grating. They vanish for gratings in cosine phase. The mean energy $E(\tau)$ (spatial integral) of the temporally integrated (duration τ) rotating grating $\tilde{g}(x, y, t)$ is thus given by

$$E(\tau) = I_0 \tau = \mathcal{F}^{-1}\big\{I_0 \tau\, \delta(f_x, f_y)\big\}. \tag{A 3}$$

For temporal integrations over rotations of multiples of 360 degrees ($E(\tau_0) = E_0$), each δ-function of the pair in equation (A 2) forms a δ-circle. The inverse Fourier transform of a δ-circle is the rotational symmetric zero-order Bessel function $J_0(r)$:

$$\mathcal{F}_{xy}^{-1}\big\{\delta(f_r - f_{r0})\big\} = 2\pi f_{r0}\, J_0(2\pi f_{r0} r) \tag{A 4}$$

with $f_{r0} = f_{x0}$, the radial frequency $f_r = (f_x^2 + f_y^2)^{1/2}$ and the radial coordinate in the space domain $r = (x^2 + y^2)^{1/2}$. Owing to the rotation, both δ-circles add up and result in the modulation

$$\tilde{m} = \tfrac{m}{2}\big[\exp(-\mathrm{i}\psi_0) + \exp(+\mathrm{i}\psi_0)\big] = m \cos\psi_0. \tag{A 5}$$

With $J_0(0) = 1$, the relation between the energy integral of the d.c. component E_0 and that of the a.c. component A_0 can be formulated by using the equations (A 3)–(A 5):

$$E_0 \tilde{m} = A_0 \iint \delta(f_r - f_{r0})\, \mathrm{d}f_x\, \mathrm{d}f_y = \mathcal{F}^{-1}\big\{A_0\, \delta(f_r - f_{r0})\big\}\big|_{r=0} = A_0 2\pi f_{r0}, \tag{A 6}$$

and thus the mean energy of the pattern is

$$E_0 = I_0 \tau_0 = A_0 2\pi f_{r0} / \tilde{m}. \tag{A 7}$$

Finally, the function $b(r)$ resulting from a rotating grating $g(x, y)$ is given by

$$b(r) = I_0 \tau_0 \left[1 + m \cos\psi_0\, J_0(2\pi f_{r0} r)\right] \tag{A 8}$$

which implies $b(r) = \text{const.}$; for example, for a phase shift of $\psi_0 = 90°$.

Appendix B

The errors resulting from the analysis of the frequency response of a system by use of a sweep signal instead of stationary harmonic signals can be approximated quite well by introducing the so-called dynamic transfer function [16]. For a harmonic signal $u_1(t) = \cos(\omega_t t)$ of the temporal angular frequency ω_t the output $u_2(t)$ of a system, with a transfer function $S(\omega_t)$, is given by

$$u_2(t) = S(\omega_t)u_1(t), \tag{B 1}$$

whereas the output $e_2(t)$ resulting from a phase-modulated signal $e_1(t) = \cos\psi(t)$ is approximated by

$$e_2(t) \cong S(\omega_{\text{inst}})e_1(t) + \tfrac{1}{2}\dot{\omega}_{\text{inst}}S''(\omega_{\text{inst}})\sin\psi(t) \tag{B 2}$$

with

$$S''(\omega_{\text{inst}}) = \mathrm{d}^2S(\omega_{\text{inst}})/\mathrm{d}\omega_{\text{inst}}^2 .$$

A comparison of the equations (B 1) and (B 2) reveals that the second term of the latter is the error ε:

$$\varepsilon = \left|\tfrac{1}{2}\dot{\omega}_{\text{inst}}S''(\omega_{\text{inst}})\right|, \tag{B 3}$$

or with equation (7),

$$\varepsilon = \left|\pi\omega^2(x/X)S''(\omega_{\text{inst}})\right|, \tag{B 4}$$

where $\omega = 2\pi n$ denotes the angular velocity of the rotating grating (cf. equation (3)). Obviously, the error depends on the second derivative of the transfer function. For the transfer function $S_S(\omega_t)$ of an ideal shutter (cf. figure 4) with the cut-off frequency ω_0

$$S_S(\omega_t) = \sin\left[\pi\omega_t/(2\omega_0)\right]/\left[\pi\omega_t/(2\omega_0)\right] = \operatorname{sinc}\left[\omega_t/(2\omega_0)\right], \tag{B 5}$$

the number of grating cycles $k_S = x/X$ defining the span within which the error is less than ε can be approximated by

$$k_S \leq (12/\pi^3)\varepsilon(\omega_0/\omega)^2 . \tag{B 6}$$

For a Gaussian lowpass

$$S_G(\omega_t) = \exp\left[-\tfrac{1}{4}\pi(\omega_t/\omega_0)^2\right], \tag{B 7}$$

the corresponding number of grating cycles k_G is

$$k_G \leq (2/\pi^2)\varepsilon(\omega_0/\omega)^2 = k_S\pi/6. \tag{B 8}$$

References

[1] Kelly, D. H., 1960, *J. opt. Soc. Am.*, **50**, 1115.
[2] Babington Smith, B., 1964, *Bull. Br. psycholog. Soc.*, **17**, 27A.
[3] Wade, N. J., 1974, *Perception*, **3**, 169.
[4] Glünder H., 1986, *Perception*, **15**, A30.
[5] Hofer-Alfeis, J., and Glünder, H., 1983, *Neue Aspekte der Informations- und Systemtheorie*, edited by R. Kersten, NTG-Fachberichte 84 (Berlin, Offenbach: VDE-Verlag), p. 315.
[6] Kelly, D. H., 1984, *J. opt. Soc. Am.* A, **1**, 107.
[7] Kelly, D. H., 1985, *J. opt. Soc. Am.* A, **2**, 216.
[8] van de Grind, W. A., Koenderink, J. J., and van Doorn, A. J., 1986, *Vision Res.*, **26**, 797.
[9] Kelly, D. H., 1961, *J. opt. Soc. Am.*, **51**, 422.

[10] Kelly, D. H., 1972, *Vision Res.*, **12**, 89.
[11] Wade, N. J., and Sanford, A. J., 1971, *Nature*, *Lond.*, **231**, 124.
[12] Marko, H., 1981, *Biol. Cybernet.*, **39**, 111.
[13] Elsner, T., 1986, Doctoral Thesis, Technische Universität München.
[14] Elsner, T., and Deubel, H., 1986, *Biol. Cybernet.*, **54**, 359.
[15] Deubel, H., and Elsner, T., 1986, *Biol. Cybernet.*, **54**, 351.
[16] Carson, J. R., and Fry, T. C., 1937, *Bell Syst. tech. J.*, **16**, 513.